Structure of Deep Eutectic Solvents (DESs): What We Know, What We Want to Know, and Why We Need to Know It

Nicole M. Stephens,[a,b,c] Emily A. Smith[a,b*]

[a] Ames Laboratory, U.S. Department of Energy, Ames, IA, 50011-3111, United States
[b] Department of Chemistry, Iowa State University, Ames, IA, 50011-3111, United States
[c] Current affiliation: Department of Biochemistry, Chemistry and Engineering Science, Wartburg College, Waverly, IA, 50677-2215, United States
* Corresponding author

Nicole M. Stephens; nicole.stephens@wartburg.edu
Emily A. Smith; esmith1@iastate.edu

Abstract

Deep eutectic solvents (DESs) are a tunable class of solvents with many advantageous properties including good thermal stability, facile synthesis, low vapor pressure, and low-to-negligible toxicity. DESs are comprised of hydrogen bond donors and acceptors that, when combined, significantly decrease the freezing point of the resulting solvent. DESs have distinct interfacial and bulk structural heterogeneity compared to traditional solvents, in part due to various intramolecular and intermolecular interactions. Many of the physiochemical properties observed for DESs are influenced by structure. However, our understanding of interfacial and bulk structure of DESs is incomplete. To fully exploit these solvents in a range of applications including catalysis, separations, and electrochemistry, a better understanding of DES structure must be obtained. In this perspective, we provide an overview of the current knowledge of interfacial and bulk structure of DESs and suggest future research directions to improve our understanding of this important information.

Introduction

The term DES refers to "liquids close to the eutectic composition of the mixtures."[1] First identified by Abbott et al.,[2, 3] deep eutectic solvents (DESs) are prepared through the appropriate combination of hydrogen bond donors (HBDs) and hydrogen bond acceptors (HBAs) resulting in a significant decrease in the freezing point of the resulting solvent compared to the pure components.[1] For example, Abbott reported the eutectic mixture of choline chloride with urea to produce choline chloride:2 urea DES with melting temperatures of 302 °C, 133 °C, and 12 °C, respectively.[4] The decrease in freezing point is attributed to extensive interspecies hydrogen bonding and charge delocalization.[1] DESs possess beneficial properties such as low vapor pressure, relatively wide liquid-range, low-to-negligible toxicity, low reactivity, and nonflammability, which make these solvents a greener alternative to traditional organic solvents.[5] Figure 1 depicts HBA and HBD structures that are mentioned in this Perspective.

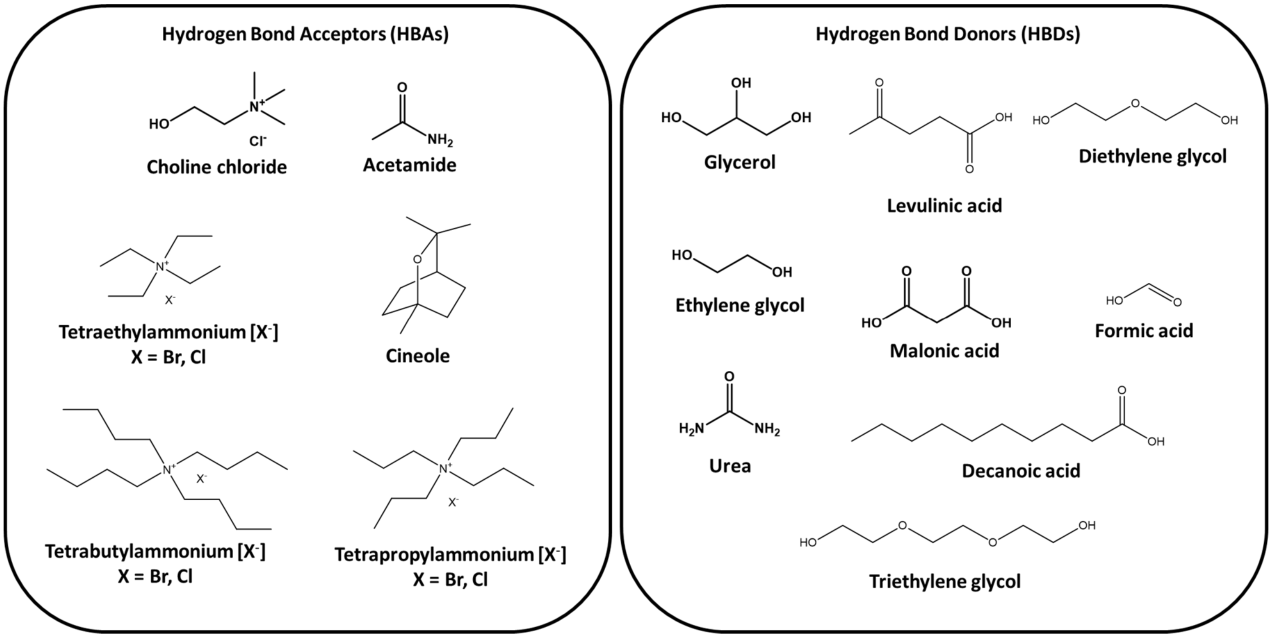

Figure 1 *Chemical structures of HBAs and HBDs mentioned in this Perspective.*

While DESs have some similar physical properties to ionic liquids (ILs), the terms DES and IL are used to refer to distinct solvents.[1, 6] ILs are typically defined as ionic compounds that have melting temperatures below 100 °C. DESs are formed through the combination of Lewis or Brønsted acids and bases, contrasting with the components of ILs which are formed through systems consisting entirely of discrete ions.[1] As opposed to ILs, DESs are generally easier and less expensive to prepare and they are considered to be greener solvents.[5] The structure (i.e., the molecular organization including intermolecular and intramolecular interactions) of DESs and ILs both at the interface and in the bulk (i.e., away from the influence of an interface) is highly dependent upon the chemical composition of the solvent and environmental properties.[7, 8] More information has been reported on the structure of ILs compared to DESs, although from available information it appears the structural organization differs with chemical structure, temperature, water content, pressure and other experimental variables.[1, 6]

In this Perspective, we discuss experimental and computational work aimed at understanding bulk and interfacial structure of DESs. In addition, we provide insight into the impact structure may have on potential applications using DESs, outline some areas where additional studies are required, and offer guidance to develop an improved understanding of the structure of DESs. We leave aside in this Perspective an exhaustive discussion of chemical and physical properties of DESs and instead refer the reader to published reviews.[1, 9-11]

Why Understanding Interfacial and Bulk Structures of DESs Matters

DESs are used in many applications that benefit from their unique characteristics, including extractions and other separations, chemical and material synthesis, catalysis, and electrochemistry.[1, 5] Knowledge of interfacial and bulk DES structure is likely to be important to optimize the use of DESs in these applications. For example, in the development of novel gas capture technologies using DESs, it is necessary to design systems that promote strong gas-solvent interactions (allowing for long gas residency times) at the gas/solvent interface.[12] Knowledge of the interfacial structure will enable designer DES systems that promote strong gas-solvent interactions.

As there is more available information about IL structure, it may provide a framework for what experimental variables may be important to DES structure.[13-15] For example, Atkin et al. utilized atomic force microscopy to show the effect of molecular composition on alkylimidazolium-based IL structure at a solid substrate (with < 100 ppm water).[15] By lengthening the alkyl chain length on the alkylimidazolium cation, a more rigid interfacial structure was induced due to the increase in solvophobic interactions that increase cohesive forces between IL layers. The orientation of the imidazolium ring was also directed towards the solid surface with increasing alkyl chain length, which produced a more favorable layering template. The authors also measured the effect of surface potential on interfacial structure. These experimental measurements also showed vastly different interfacial structures alter the task-specific efficiency of an IL in the field of electrochemistry.

In addition to structural ordering at a solid interface, both ILs and DESs exhibit unique structure in the bulk, away from the influence of an interface, compared to traditional solvents. Bulk structure of ILs is defined by the manner in which ions organize. In many cases this organization leads to polar and nonpolar domains, with structural ordering over lengths scales from approximately a nanometer to tens of nanometers depending on the ILs.[7, 16] Bulk IL structure has been strategically tuned for the synthesis of metal nanoparticles of discrete sizes.[17] Santini et al. utilized both computational and experimental results to demonstrate the controlled size of ruthenium nanoparticles synthesized in alkylimidazolium ILs (298 K, 0.4 MPa).[17] Their work indicated nanoparticle growth was occurring within the nonpolar domains of the IL and thus, the size of the nanoparticle can be tuned by exploiting the tunable size of the nonpolar domains.[17]

Based on the impact IL structure has on electrochemical reactions, nanoparticle synthesis and numerous other applications,[18-20] as well as some available information for DESs, it is logical to conclude structure may play a critical role in many applications using DESs. In the following sections, we discuss the computational and experimental studies of interfacial (gas/DES, liquid/DES, and solid/DES) and bulk DES structure as a function of experimental variables that impact structure. For example, at a low water concentration (<40 wt%), measurable structure is obtained for a DES; however, at high water contents, the structure of a DES completely dissipates.[21]

Computational Modeling of Interfacial and Bulk Structure in DESs

Investigations of DES structure through computational modeling can provide insight into structural features that may not be experimentally measurable or provide information on a greater diversity of DES compositions.[17] Yet, DES are complex and present challenges to computational modeling.[22]

Bulk DES Structure

The structure of DESs in the bulk can be tuned by adjusting the molecular composition of the DES components.[23-28] In common choline chloride-based DESs (333 K), increasing concentration of HBA results in decreased hydrogen bonding between HBD molecules, an increase in molecular mobility of the HBD, and nanoscopic structural heterogeneities.[29] By elongating the alkyl side chains or increasing the number of hydroxyl groups on the choline chloride, Kirchner et al. demonstrated the ability to increase the structural heterogeneity within a DES (423.15 K, Figure 2).[30] This may assist with applications such as template-assisted synthesis. Kashyap et al. utilized molecular dynamics simulations to elucidate what they termed short-range ordering (interactions between DES components at less than 1 nm distance) and long-range ordering (interactions between DES components at greater than 1 nm distance) of both choline chloride:2 ethylene glycol and choline chloride:2 urea (303 K, 1 bar).[23, 27] A strong hydrogen bonding network with HBDs aligning in various conformations was identified in both systems. The HBD disrupts electrostatic interactions of the HBA, but the electrostatic interactions remain sufficient to induce a unique long-range structural organization.[23, 27]

Alterations in DES structure can be correlated with alterations in physiochemical properties. The formation of a stronger hydrogen bonding network in choline chloride:2 urea causes a large melting point depression as well as an elevated viscosity compared to choline chloride:2 glycerol and choline chloride:2 ethylene glycol.[25] Comparing the latter DESs composed of polyols, a higher viscosity was noted in choline chloride:2 glycerol due to the excess of groups on the HBD capable of participating in hydrogen bonding and more extensive HBD self-interaction.[25]

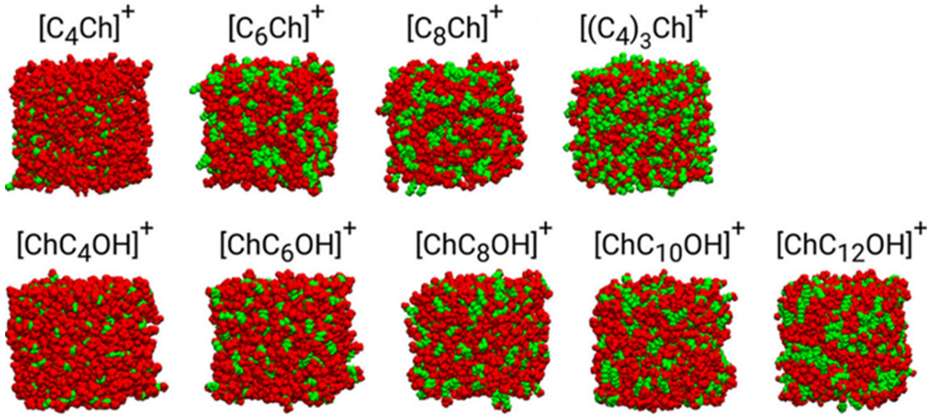

Figure 2 *Space-filling representation of the classical molecular dynamics simulation boxes for choline chloride and choline chloride-derivatives. Color codes indicate polar groups (red) and nonpolar groups (green).* Ch^+ *indicates the choline cation,* C_nCh^+ *indicates the alkyl-modified choline cation, and* ChC_nOH^+ *indicates the alkyl- and hydroxyl-modified choline cation. Structural heterogeneity is visible for the systems with side chain lengths of eight carbon units or*

more. Structural heterogeneity is more pronounced with increasing alkyl chain length than hydroxyl-substituted side chain choline chloride-based compounds. Reprinted with permission from reference 30. Copyright 2019 Wiley.

Gas/DES Interfacial Structure

A few computational models of the structure at the gas/DES interface provide beneficial information for gas capture and separation technologies.[12, 31-35] Aparicio et al. noted the HBDs in choline chloride:2 urea and choline chloride:malonic acid (318 K, 0.1 MPa) are oriented parallel to the gas/DES interface. The HBD in choline chloride:2 glycerol is oriented slightly off parallel, although an exact angle was not provided.[33] In choline chloride:levulinic acid (298 – 348 K, 0.1 MPa), the choline chloride (HBA) is oriented parallel and farther away from the interface compared to the levulinic acid (HBD), which is oriented perpendicular to the interface and is involved in strong intermolecular interactions with gas molecules.[34] Interestingly, in cineole-based DESs (303 K, 1 bar), the HBA orients closer to the gas/DES interface leading to local phase separation and an induced heterogeneity that could affect gas solubility and diffusivity.[32] In all studied systems, the structure of the DES at the gas/DES interface resulted from a reorganization that maximizes gas/DES interactions.[32-34]

Liquid/DES Interfacial Structure

As with the gas/DES interface, molecular dynamics simulations show liquid/DES interfacial structure is dictated by an alignment that maximizes intermolecular interactions between the liquid and DES. For an *n*-octane/hydrophobic tetrabutylammonium bromide:formic acid DES interface (303 K, 0.1 MPa) , HBA ions are farther away from the interface while HBD molecules pack closely at the interface and interact with *n*-octane[36] For the same HBA (with a different halide anion) and a more nonpolar decanoic acid HBD (323 – 363 K), molecular dynamics simulations of the water/DES interface show similar results.[37] Shao et al. identified three key reasons for a non-bulk-like DES structure at the interface (295 K, 1 atm): (1) distribution of DES components at the interface in order to maximize intermolecular interactions between DES components and water, (2) dipole fluctuations at the interface, and (3) the three types of hydrogen bonding interactions that can occur at the interface (DES-DES, DES-water, water-water).[38] For the various hydrophobic-DESs studied by Shao et al.,[38] the interfacial region ranged from 1.6 to 2.2 nm; in this region, simulations from multiple authors suggest that a slight mixing of DES and liquid occurs.[36-38]

Solid/DES Interfacial Structure

Molecular dynamics simulations have indicated a more ordered structure at the solid/DES interface compared with the liquid/DES and air/DES interface, with significant DES densification in the interfacial region.[39-41] Simulations of choline chloride-based DESs (403 K, 1 bar) with commonly investigated HBDs have revealed the HBA and HBD form a parallel arrangement to a graphene surface; however, the HBA cation experiences strong intermolecular interactions with the surface, whereas weaker interactions with the HBD are present.[40] This was similar to reported simulations of various common DESs (298 K) at the highly ordered pyrolytic graphite surface.[42] Under all simulated surface potentials, HBD molecules were repelled from the surface while HBA molecules showed strong interactions with the surface. In addition, Atkin et al. indicated the extent of layering is dependent not only upon the surface potential but also upon the HBD's hydrogen bonding capacity; stronger cohesive interactions can exist between adjacent layers with increasing hydrogen bonding capacity.[42] Many simulations have indicated the size of the solid/DES interfacial region is on the order of a few angstroms at the graphene and graphite surface, and surface effects that alter DES structure (from that of the bulk) disappear after ~10 Å.[40, 42] This is smaller in size than reported for solid/liquid interfacial regions for ILs on a mica surface,[43] although there is considerable variation reported for ILs.[44-47]

Measurements of Interfacial and Bulk Structure in DESs

Measurements of interfacial and bulk structure in DESs have been performed using direct (measuring structure itself) and indirect methods (measurement of a property influenced by structure). One indirect measurement is molecular diffusion, which is related to solvent structure under some conditions. Indirect measurements have been used primarily to elucidate structural heterogeneities in the bulk. Structural information, both at the interface and in the bulk, has been more commonly reported for direct measurements, including atomic force microscopy and sum frequency generation.[48-50]

Bulk DES Structure

Although the constituents of the DES play a significant role in its structure, general trends can be found in published data for different types of DESs.[24, 26, 51-54] Edler et al. conducted extensive work to elucidate the bulk structure of many different classes of DESs via various scattering techniques.[24, 51, 52] For example, the bulk structure of choline chloride:2 urea (2252 ppm water) showed structural ordering with an approximate 10 Å scale using neutron scattering.[24] Neutron scanning experiments of choline chloride:2 glycerol (269 – 318 K) revealed structural ordering on the same length scale; the size of this structure was consistent with the average distance between ionic (choline chloride) and molecular domains (glycerol) from molecular dynamics simulations.[53] Utilizing fluorescence correlation spectroscopy and other fluorescence techniques, diffusion-viscosity decoupling due to structural heterogeneities in the bulk acetamide-based and tetraalkylammonium-based DESs and other DESs has been revealed (temperature varies by study ranging from 298 – 358 K).[55-58] In the case of tetraalkylammonium-based DESs (298 K, ca. 0.1 wt% water), the spatial and dynamic heterogeneities become increasingly larger with increasing alkyl chain length on the HBA cation.[57] Self-diffusion coefficients probed via pulsed gradient field nuclear magnetic resonance of choline chloride-based DESs (298/333 K) revealed the selection of HBD played a significant role in the overall mobility of the DESs.[59] While some selected HBDs diffused faster than the HBA, other HBDs diffused slower; restricted mobility was correlated with the formation of structural heterogeneities.

Interfacial Structure in DESs

Many measurements at the solid/DES interface show structure that is dependent upon surface composition, surface charge, and DES composition.[42, 60, 61] Comparing the formation of interfacial structure on mica and a highly ordered pyrolytic graphite interface of the same DES (293 K, 0.27 wt% water), Christofferson et al. noted remarkable differences (Figure 3).[61] While both systems showed well-ordered lateral structures, the adsorbed layer at the mica interface had a distinct rhomboidal symmetry that was composed of all DES constituents.[61] At the highly ordered pyrolytic graphite interface, however, the adsorbed layer was less structured with no specific orientation with respect to the surface and measurements indicated an excess of molecular species at the surface.[61] Atomic force microscopy revealed only a single interfacial layer of less than 1 nm for choline chloride-based DESs (0.34 wt% water).[62] The ordering of this layer was determined to be surface potential-dependent and the ordering was more pronounced at more positive potentials due to ion templating. Structural heterogeneities are even more pronounced at the solid/DES interface for less commonly studied amphiphilic DESs as measured by atomic force microscopy.[60] Interfacial structure becomes larger and better defined with increasing alkyl chain length due to the increased solvophobic interactions. Near-surface layers were also observed to extend farther into the bulk with increasing alkyl chain length.

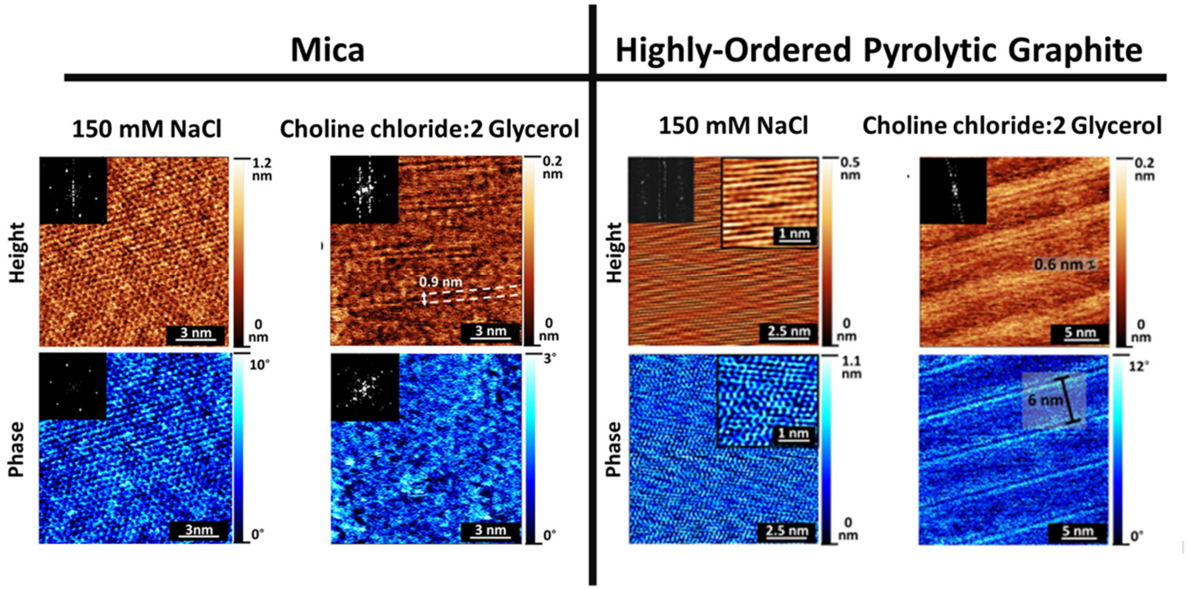

Figure 3 *Height and phase images of choline chloride:2 glycerol and 150 mM NaCl (conventional electrolyte used as a control system) at mica and highly-ordered pyrolytic graphite interfaces as measured by amplitude modulated-atomic force microscopy. Height and phase images collected of NaCl on mica and highly-ordered pyrolytic graphite were utilized to confirm interfacial measurements of DES are indicative of surface-absorbed species rather than the underlying substrate itself. On the mica surface, the absorbed DES layer has a rhomboidal symmetry with a repeating spacing of ~0.9 nm (inset 2D-fast Fourier transform image) composed of all DES species (as determined by subsequent molecular dynamic simulations). On the highly-ordered pyrolytic graphite surface, the absorbed DES layer forms apolar-driven row-like structure with repeating spacing of ~0.6 nm (inset 2D-fast Fourier transform image) composed with a composition that excludes the chloride ion (as determined by subsequent*

molecular dynamic simulations). Features spaced at 6 nm distances are indicative of grain boundaries which are amplified in the presence of DES. Figure adapted with permission from reference 61. Copyright 2021 Elsevier.

Effect of Water Content on Interfacial and Bulk Structure in DESs

Many DESs contain water, and even when dried to remove water, a trace amount of water is an unavoidable impurity.[63] There are a few reports of bulk DES structure as a function of water content and fewer reports of interfacial structure.[21, 37, 38, 62, 64-73]

Bulk DES Structure

Via molecular dynamics simulations, Kashyap et al. noted that the structure of choline chloride:2 urea was retained up to 41 wt% water (303 K).[21] With 58.1 wt% water an aqueous solution of choline chloride:2 urea was formed with water molecules preferentially solvating the chloride anions and the ammonium group of the choline cation (Figure 4); thus, water is acting as a secondary HBD/HBA competing with urea for hydrogen bonding and electrostatic interactions. The preservation of DES structure with increasing incorporated water was also found for other HBD/HBA combinations including choline chloride:2 ethylene glycol (303 K, 14.3 to 87 wt% water).[69] Spreti et al. utilized Fourier transform infrared and nuclear magnetic resonance spectroscopy to show choline chloride:glycol-based DES bulk structural ordering was reduced but still detectable up to 50 wt% water at 98 K, however, the structure was dissolved at around 75 wt% water.[68] The overall structure of the DES was also maintained at high water contents when the HBD had an increase in oxyethylene groups.

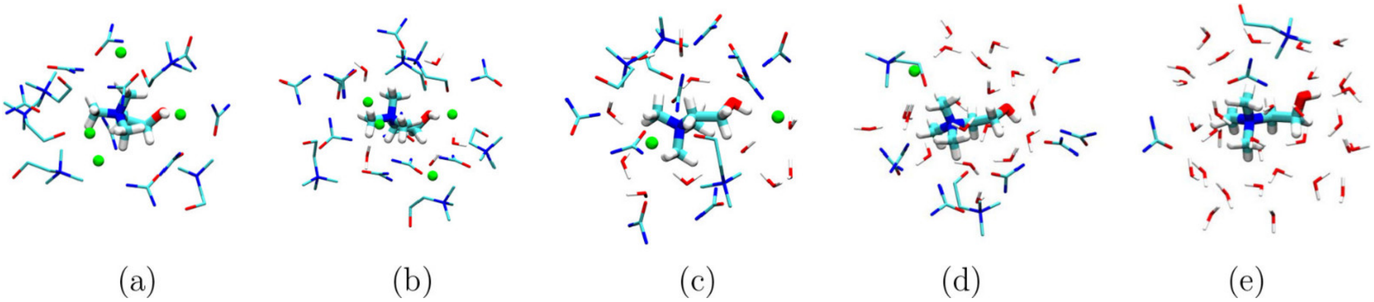

Figure 4 *Molecular representation of the arrangement of choline cations, chloride anions, urea, and water around a distance of 4 Å from a central choline cation for (a) choline chloride:2 urea, and choline chloride:2 urea with: (b) 3.4 wt% water, (c) 21.7 wt% water, (d) 41 wt%, and (e) 58.1 wt%. In each snapshot, nitrogen, oxygen, carbon, and hydrogen atoms are shown as blue, red, cyan, and white stick, respectively. Chloride anions are rendered as green spheres. Reprinted with permission from Reference 21. Copyright 2018 American Chemical Society.*

Interfacial Structure

Experimental data show that interfacial structure, similar to bulk structure, is retained at high water contents.[62, 66] At the gas/DES interface, Bakker et al. observed a gradual depletion of urea as well as enrichment and alignment of choline cations at the surface with increasing water contents up to 40 wt%..[66] At 60 wt% water, the interfacial structure of the DES is indistinguishable from that of pure water. This phenomenon was also observed using atomic force microscopy force-distance curves at the solid/DES interface with 30-50 wt% water.[62] The interfacial structure is similar to that of a salt solution up to 40 wt% water and with increasing water the interfacial structure steadily decreases.

Main Challenges in Understanding Interfacial and Bulk Structure

Despite the many applications using DESs where structure is expected to have an important role, not a lot is known about the interfacial or bulk DES structure at relevant conditions for these applications. There is a nearly infinite number of DESs and experimental conditions possible. General structural trends may be found in existing data, and this may be aided in the future using machine learning and other advanced data analytics methods, but these properties should ideally be investigated for each DES and experimental conditions relevant to applications using these solvents.

Computational studies provide details of DES structure; however, experimental data often used in these computational models vary widely. For example, the melting point of choline chloride:2 urea varies in the literature from 12 °C (0.652 wt% water)[74] to 24 °C (0.200 wt% water).[75] These differences in reported values could be due to a variety of reasons including sample preparation, storage of these hygroscopic materials, impurities and others. This shows the importance of controlling and reporting all experimental variables for DES studies.

Accurate, reproducible, and fast methods to measure DES structure, particularly interfacial structure, are needed that could further our understanding. Previously, total internal reflection fluorescence spectroscopy coupled with a viscosity-sensitive fluorescent probe was used to show significant structural ordering at the solid/IL interface.[76] Using this method, Nishi et al. detected a solid-like highly-viscous region at the solid/IL interface that was estimated to be 40 times more viscous than the bulk solution.[76] Extending this method to explore interfacial regions in DES may be beneficial. For example, detection of solid/DES interfacial structure could have strong implications on the effectiveness of DESs for applications in which mass transfer rates greatly dictate performance.

With the successful application of a variety DESs as chromatographic media,[74, 77, 78] studies conducted to understand interfacial structure can lead to more efficient design of DESs as separation media. Interfacial interactions, important to separations, can be impacted by DES interfacial structure, which thus dictate performance of a DES chromatographic system. Future studies should aim to correlate interfacial structure with additional components, such as encountered in real systems using DESs. For example, single molecule microscopy has been previously used to probe mixed-mode sorption phenomena of a cationic dye at the interface of C_{18} and an aqueous solution of acetonitrile, which models reverse-phase liquid chromatographic conditions and can explain chromatographic behavior.[79] Investigations of interfacial interactions utilizing techniques such as fluorescence correlation spectroscopy and single molecule microscopy can provide beneficial interaction information that can directly indicate performance of a DES chromatographic system.

Conclusions

In this Perspective, we have provided a review of experimental and computational work reported on bulk and interfacial structure of DESs as well as offered insight into the impact structure may have on current and future applications of DESs. Future research will provide information that enables the design of DESs that have favorable bulk and/or interfacial structure that will improve the implementation of DESs in various systems including separations, catalysis, energy storage, among many other yet to be developed applications.

Acknowledgements

This research was funded by U.S. Department of Energy (DOE), Office of Science, Basic Energy Sciences, Division of Chemical Sciences, Geosciences, and Biosciences. Ames Laboratory is operated for the DOE under Contract No. DE-AC02-07CH11358.

References

(1) Smith, E. L.; Abbott, A. P.; Ryder, K. S. Deep Eutectic Solvents (Dess) and Their Applications. *Chem. Rev.* **2014**, *114,* 11060-11082.
(2) Abbott, A. P.; Capper, G.; Davies, D. L.; Munro, H. L.; Rasheed, R. K.; Tambyrajah, V. Preparation of Novel, Moisture-Stable, Lewis-Acidic Ionic Liquids Containing Quaternary Ammonium Salts with Functional Side Chains. *Chem. Comm.* **2001**, 2010-2011.
(3) Abbott, A. P.; Boothby, D.; Capper, G.; Davies, D. L.; Rasheed, R. K. Deep Eutectic Solvents Formed between Choline Chloride and Carboxylic Acids: Versatile Alternatives to Ionic Liquids. *J. Am. Chem. Soc.* **2004**, *126,* 9142-9147.
(4) Abbott, A. P.; Capper, G.; Davies, D. L.; Rasheed, R. K.; Tambyrajah, V. Novel Solvent Properties of Choline Chloride/Urea Mixtures. *Chem. Comm.* **2003**, 70-71.
(5) Zhang, Q.; De Oliveira Vigier, K.; Royer, S.; Jérôme, F. Deep Eutectic Solvents: Syntheses, Properties and Applications. *Chem. Soc. Rev.* **2012**, *41,* 7108-7146.
(6) Płotka-Wasylka, J.; de la Guardia, M.; Andruch, V.; Vilková, M. Deep Eutectic Solvents Vs Ionic Liquids: Similarities and Differences. *Microchem. J.* **2020**, *159,* 105539.
(7) Hayes, R.; Warr, G. G.; Atkin, R. Structure and Nanostructure in Ionic Liquids. *Chem. Rev.* **2015**, *115,* 6357-6426.
(8) Kaur, S.; Kumari, M.; Kashyap, H. K. Microstructure of Deep Eutectic Solvents: Current Understanding and Challenges. *J. Phys. Chem. B* **2020**, *124,* 10601-10616.
(9) El Achkar, T.; Greige-Gerges, H.; Fourmentin, S. Basics and Properties of Deep Eutectic Solvents: A Review. *Environ Chem Lett.* **2021**, *19,* 3397-3408.
(10) Hansen, B. B.; Spittle, S.; Chen, B.; Poe, D.; Zhang, Y.; Klein, J. M.; Horton, A.; Adhikari, L.; Zelovich, T.; Doherty, B. W.; et al. Deep Eutectic Solvents: A Review of Fundamentals and Applications. *Chem. Rev.* **2021**, *121,* 1232-1285.
(11) Liu, Y.; Friesen, J. B.; McAlpine, J. B.; Lankin, D. C.; Chen, S.-N.; Pauli, G. F. Natural Deep Eutectic Solvents: Properties, Applications, and Perspectives. *J. Nat. Prod.* **2018**, *81,* 679-690.

(12) Shen, Y.; Abedin, R.; Hung, F. R. On the Performance of Confined Deep Eutectic Solvents and Ionic Liquids for Separations of Carbon Dioxide from Methane: Molecular Dynamics Simulations. *Langmuir* **2019**, *35,* 3658-3671.
(13) Minami, I. Ionic Liquids in Tribology. *Molecules* **2009**, *14,* 2286-2305.
(14) Minami, I.; Kamimura, H.; Mori, S. Thermo-Oxidative Stability of Ionic Liquids as Lubricating Fluids. *J. Synth. Lubr.* **2007**, *24,* 135-147.
(15) Li, H.; Endres, F.; Atkin, R. Effect of Alkyl Chain Length and Anion Species on the Interfacial Nanostructure of Ionic Liquids at the Au(111)–Ionic Liquid Interface as a Function of Potential. *Phys. Chem. Chem. Phys.* **2013**, *15,* 14624-14633.
(16) Wang, Y.-L.; Li, B.; Sarman, S.; Mocci, F.; Lu, Z.-Y.; Yuan, J.; Laaksonen, A.; Fayer, M. D. Microstructural and Dynamical Heterogeneities in Ionic Liquids. *Chem. Rev.* **2020**, *120,* 5798-5877.
(17) Gutel, T.; Santini, C. C.; Philippot, K.; Padua, A.; Pelzer, K.; Chaudret, B.; Chauvin, Y.; Basset, J.-M. Organized 3d-Alkyl Imidazolium Ionic Liquids Could Be Used to Control the Size of in Situ Generated Ruthenium Nanoparticles? *J. Mater. Chem.* **2009**, *19,* 3624-3631.
(18) Liu, J.-f.; Jiang, G.-b.; Liu, J.-f.; Jönsson, J. Å. Application of Ionic Liquids in Analytical Chemistry. *TrAC, Trends Anal. Chem.* **2005**, *24,* 20-27.
(19) MacFarlane, D. R.; Tachikawa, N.; Forsyth, M.; Pringle, J. M.; Howlett, P. C.; Elliott, G. D.; Davis, J. H.; Watanabe, M.; Simon, P.; Angell, C. A. Energy Applications of Ionic Liquids. *Energy Environ. Sci.* **2014**, *7,* 232-250.
(20) Plechkova, N. V.; Seddon, K. R. Applications of Ionic Liquids in the Chemical Industry. *Chem. Soc. Rev.* **2008**, *37,* 123-150.
(21) Kumari, P.; Shobhna; Kaur, S.; Kashyap, H. K. Influence of Hydration on the Structure of Reline Deep Eutectic Solvent: A Molecular Dynamics Study. *ACS Omega* **2018**, *3,* 15246-15255.
(22) Velez, C.; Acevedo, O. Simulation of Deep Eutectic Solvents: Progress to Promises. *Wiley Interdiscip. Rev. Comput. Mol. Sci.* **2022**, e1598.
(23) Kaur, S.; Sharma, S.; Kashyap, H. K. Bulk and Interfacial Structures of Reline Deep Eutectic Solvent: A Molecular Dynamics Study. *J. Chem. Phys.* **2017**, *147,* 194507.
(24) Hammond, O. S.; Bowron, D. T.; Edler, K. J. Liquid Structure of the Choline Chloride-Urea Deep Eutectic Solvent (Reline) from Neutron Diffraction and Atomistic Modelling. *Green Chem.* **2016**, *18,* 2736-2744.
(25) Stefanovic, R.; Ludwig, M.; Webber, G. B.; Atkin, R.; Page, A. J. Nanostructure, Hydrogen Bonding and Rheology in Choline Chloride Deep Eutectic Solvents as a Function of the Hydrogen Bond Donor. *Phys. Chem. Chem. Phys.* **2017**, *19,* 3297-3306.
(26) Zhang, Y.; Poe, D.; Heroux, L.; Squire, H.; Doherty, B. W.; Long, Z.; Dadmun, M.; Gurkan, B.; Tuckerman, M. E.; Maginn, E. J. Liquid Structure and Transport Properties of the Deep Eutectic Solvent Ethaline. *J. Phys. Chem. B* **2020**, *124,* 5251-5264.
(27) Kaur, S.; Malik, A.; Kashyap, H. K. Anatomy of Microscopic Structure of Ethaline Deep Eutectic Solvent Decoded through Molecular Dynamics Simulations. *J. Phys. Chem. B* **2019**, *123,* 8291-8299.
(28) Ferreira, E. S. C.; Voroshylova, I. V.; Figueiredo, N. M.; Pereira, C. M.; Cordeiro, M. N. D. S. Computational and Experimental Study of Propeline: A Choline Chloride Based Deep Eutectic Solvent. *J. Mol. Liq.* **2020**, *298,* 111978.

(29) Spittle, S.; Poe, D.; Doherty, B.; Kolodziej, C.; Heroux, L.; Haque, M. A.; Squire, H.; Cosby, T.; Zhang, Y.; Fraenza, C.; et al. Evolution of Microscopic Heterogeneity and Dynamics in Choline Chloride-Based Deep Eutectic Solvents. *Nat. Commun.* **2022**, *13,* 219.
(30) Alizadeh, V.; Geller, D.; Malberg, F.; Sánchez, P. B.; Padua, A.; Kirchner, B. Strong Microheterogeneity in Novel Deep Eutectic Solvents. *ChemPhysChem* **2019**, *20,* 1786-1792.
(31) Heydari Dokoohaki, M.; Zolghadr, A. R. Significant Improvement in Co2 Absorption by Deep Eutectic Solvents as Immobilized Sorbents: Computational Analysis. *J. Phys. Chem. B* **2021**, *125,* 10035-10046.
(32) Rozas, S.; Atilhan, M.; Aparicio, S. Bulk Liquid Phase and Interfacial Behavior of Cineole–Based Deep Eutectic Solvents with Regard to Carbon Dioxide. *J. Mol. Liq.* **2022**, *353,* 118748.
(33) Garcia, G.; Atilhan, M.; Aparicio, S. Interfacial Properties of Deep Eutectic Solvents Regarding to Co2 Capture. *J. Phys. Chem. C* **2015**, *119,* 21413-21425.
(34) Ullah, R.; Atilhan, M.; Anaya, B.; Khraisheh, M.; García, G.; ElKhattat, A.; Tariq, M.; Aparicio, S. A Detailed Study of Cholinium Chloride and Levulinic Acid Deep Eutectic Solvent System for Co 2 Capture Via Experimental and Molecular Simulation Approaches. *Phys. Chem. Chem. Phys.* **2015**, *17,* 20941-20960.
(35) Felipe, A.; Lovenduski, C.; Baker, J. L.; Lindberg, G. E. Long-Ranged Heterogeneous Structure in Aqueous Solutions of the Deep Eutectic Solvent Choline and Geranate at the Liquid-Vapor Interface. *Phys. Chem. Chem. Phys.* **2022**, *24*, 13720-13729.
(36) Gutiérrez, A.; Atilhan, M.; Aparicio, S. Theoretical Study of Oil Desulfuration by Ammonium-Based Deep Eutectic Solvents. *Energy Fuels* **2018**, *32,* 7497-7507.
(37) Salehi, H. S.; Moultos, O. A.; Vlugt, T. J. Interfacial Properties of Hydrophobic Deep Eutectic Solvents with Water. *J. Phys. Chem. B* **2021**, *125,* 12303-12314.
(38) Abbas, U. L.; Qiao, Q.; Nguyen, M. T.; Shi, J.; Shao, Q. Structure and Hydrogen Bonds of Hydrophobic Deep Eutectic Solvent-Aqueous Liquid–Liquid Interfaces. *AIChE J.* **2021**, *67,* e17427.
(39) Atilhan, M.; Aparicio, S. Molecular Dynamics Simulations of Mixed Deep Eutectic Solvents and Their Interaction with Nanomaterials. *J. Mol. Liq.* **2019**, *283,* 147-154.
(40) Atilhan, M.; Costa, L. T.; Aparicio, S. Elucidating the Properties of Graphene–Deep Eutectic Solvents Interface. *Langmuir* **2017**, *33,* 5154-5165.
(41) Rozas, S.; Atilhan, M.; Aparicio, S. Deep Eutectic Solvent Reline at 2d Nanomaterial Interfaces. *J. Phys. Chem. B* **2020**, *124,* 1197-1206.
(42) Chen, Z.; McLean, B.; Ludwig, M.; Stefanovic, R.; Warr, G. G.; Webber, G. B.; Page, A. J.; Atkin, R. Nanostructure of Deep Eutectic Solvents at Graphite Electrode Interfaces as a Function of Potential. *J. Phys. Chem. C* **2016**, *120,* 2225-2233.
(43) Cheng, H. W.; Weiss, H.; Stock, P.; Chen, Y. J.; Reinecke, C. R.; Dienemann, J. N.; Mezger, M.; Valtiner, M. Effect of Concentration on the Interfacial and Bulk Structure of Ionic Liquids in Aqueous Solution. *Langmuir* **2018**, *34,* 2637-2646.
(44) Gil, P. S.; Jorgenson, S. J.; Riet, A. R.; Lacks, D. J. Relationships between Molecular Structure, Interfacial Structure, and Dynamics of Ionic Liquids near Neutral and Charged Surfaces. *J. Phys. Chem. C* **2018**, *122,* 27462-27468.
(45) Wang, S.; Li, S.; Cao, Z.; Yan, T. Molecular Dynamic Simulations of Ionic Liquids at Graphite Surface. *J. Phys. Chem. C* **2010**, *114,* 990-995.
(46) Begić, S.; Jónsson, E.; Chen, F.; Forsyth, M. Molecular Dynamics Simulations of Pyrrolidinium and Imidazolium Ionic Liquids at Graphene Interfaces. *Phys. Chem. Chem. Phys.* **2017**, *19,* 30010-30020.

(47) Wang, Y.; Tian, G. The Influence of Anion Structure on the Ionic Liquids/Au (100) Interface by Molecular Dynamics Simulations. *Langmuir* **2021**, *37,* 14059-14071.
(48) Chen, Z.; Li, Z.; Zhao, W.; Matsumoto, R. A.; Thompson, M. W.; Morales-Collazo, O.; Cummings, P. T.; Mangolini, F.; Brennecke, J. F. Investigation of Multilayered Structures of Ionic Liquids on Graphite and Platinum Using Atomic Force Microscopy and Molecular Simulations. *Langmuir* **2022**, *38,* 4036-4047.
(49) Baldelli, S. Interfacial Structure of Room-Temperature Ionic Liquids at the Solid–Liquid Interface as Probed by Sum Frequency Generation Spectroscopy. *J. Phys. Chem. Lett.* **2013**, *4,* 244-252.
(50) Labuda, A.; Grütter, P. Atomic Force Microscopy in Viscous Ionic Liquids. *Langmuir* **2012**, *28,* 5319-5322.
(51) Hammond, O. S.; Bowron, D. T.; Jackson, A. J.; Arnold, T.; Sanchez-Fernandez, A.; Tsapatsaris, N.; Garcia Sakai, V.; Edler, K. J. Resilience of Malic Acid Natural Deep Eutectic Solvent Nanostructure to Solidification and Hydration. *J. Phys. Chem. B* **2017**, *121,* 7473-7483.
(52) Hammond, O. S.; Bowron, D. T.; Edler, K. J. Structure and Properties of "Type Iv" Lanthanide Nitrate Hydrate:Urea Deep Eutectic Solvents. *ACS Sustainable Chem. Eng.* **2019**, *7,* 4932-4940.
(53) Faraone, A.; Wagle, D. V.; Baker, G. A.; Novak, E. C.; Ohl, M.; Reuter, D.; Lunkenheimer, P.; Loidl, A.; Mamontov, E. Glycerol Hydrogen-Bonding Network Dominates Structure and Collective Dynamics in a Deep Eutectic Solvent. *J. Phys. Chem. B* **2018**, *122,* 1261-1267.
(54) Cui, Y.; Rushing, J. C.; Seifert, S.; Bedford, N. M.; Kuroda, D. G. Molecularly Heterogeneous Structure of a Nonionic Deep Eutectic Solvent Composed of N-Methylacetamide and Lauric Acid. *J. Phys. Chem. B* **2019**, *123,* 3984-3993.
(55) Subba, N.; Das, N.; Sen, P. Partial Viscosity Decoupling of Solute Solvation, Rotation, and Translation Dynamics in Lauric Acid/Menthol Deep Eutectic Solvent: Modulation of Dynamic Heterogeneity with Length Scale. *J. Phys. Chem. B* **2020**, *124,* 6875-6884.
(56) Subba, N.; Tarif, E.; Sen, P.; Biswas, R. Subpicosecond Solvation Response and Partial Viscosity Decoupling of Solute Diffusion in Ionic Acetamide Deep Eutectic Solvents: Fluorescence up-Conversion and Fluorescence Correlation Spectroscopic Measurements. *J. Phys. Chem. B* **2020**, *124,* 1995-2005.
(57) Hossain, S. S.; Paul, S.; Samanta, A. Liquid Structure and Dynamics of Tetraalkylammonium Bromide-Based Deep Eutectic Solvents: Effect of Cation Chain Length. *J. Phys. Chem. B* **2019**, *123,* 6842-6850.
(58) Subba, N.; Polok, K.; Piatkowski, P.; Ratajska-Gadomska, B.; Biswas, R.; Gadomski, W.; Sen, P. Temperature-Dependent Ultrafast Solvation Response and Solute Diffusion in Acetamide–Urea Deep Eutectic Solvent. *J. Phys. Chem. B* **2019**, *123,* 9212-9221.
(59) D'Agostino, C.; Harris, R. C.; Abbott, A. P.; Gladden, L. F.; Mantle, M. D. Molecular Motion and Ion Diffusion in Choline Chloride Based Deep Eutectic Solvents Studied by 1h Pulsed Field Gradient Nmr Spectroscopy. *Phys. Chem. Chem. Phys.* **2011**, *13,* 21383-21391.
(60) Buzolic, J. J.; Li, H.; Aman, Z. M.; Warr, G. G.; Atkin, R. Self-Assembled Nanostructure Induced in Deep Eutectic Solvents Via an Amphiphilic Hydrogen Bond Donor. *J. Colloid Interface Sci.* **2022**, *616,* 121-128.
(61) Elbourne, A.; Meftahi, N.; Greaves, T. L.; McConville, C. F.; Bryant, G.; Bryant, S. J.; Christofferson, A. J. Nanostructure of a Deep Eutectic Solvent at Solid Interfaces. *J. Colloid Interface Sci.* **2021**, *591,* 38-51.

(62) Hammond, O. S.; Li, H.; Westermann, C.; Al-Murshedi, A. Y. M.; Endres, F.; Abbott, A. P.; Warr, G. G.; Edler, K. J.; Atkin, R. Nanostructure of the Deep Eutectic Solvent/Platinum Electrode Interface as a Function of Potential and Water Content. *Nanoscale Horiz.* **2019**, *4,* 158-168.
(63) Ma, C.; Laaksonen, A.; Liu, C.; Lu, X.; Ji, X. The Peculiar Effect of Water on Ionic Liquids and Deep Eutectic Solvents. *Chem. Soc. Rev.* **2018**, *47,* 8685-8720.
(64) Busato, M.; Di Lisio, V.; Del Giudice, A.; Tomai, P.; Migliorati, V.; Galantini, L.; Gentili, A.; Martinelli, A.; D'Angelo, P. Transition from Molecular-to Nano-Scale Segregation in a Deep Eutectic Solvent-Water Mixture. *J. Mol. Liq.* **2021**, *331,* 115747.
(65) Panda, S.; Kundu, K.; Kiefer, J.; Umapathy, S.; Gardas, R. L. Molecular-Level Insights into the Microstructure of a Hydrated and Nanoconfined Deep Eutectic Solvent. *J. Phys. Chem. B* **2019**, *123,* 3359-3371.
(66) Gera, R.; Moll, C. J.; Bhattacherjee, A.; Bakker, H. J. Water-Induced Restructuring of the Surface of a Deep Eutectic Solvent. *J. Phys. Chem. Lett.* **2022**, *13,* 634-641.
(67) Liu, S.; Tan, Z.; Wu, J.; Mao, B.; Yan, J. Electrochemical Interfaces in Ionic Liquids/Deep Eutectic Solvents Incorporated with Water: A Review. *J. Electrochem. Sci. Technol. n/a,* e2100199.
(68) Gabriele, F.; Chiarini, M.; Germani, R.; Tiecco, M.; Spreti, N. Effect of Water Addition on Choline Chloride/Glycol Deep Eutectic Solvents: Characterization of Their Structural and Physicochemical Properties. *J. Mol. Liq.* **2019**, *291,* 111301.
(69) Kaur, S.; Gupta, A.; Kashyap, H. K. How Hydration Affects the Microscopic Structural Morphology in a Deep Eutectic Solvent. *J. Phys. Chem. B* **2020**, *124,* 2230-2237.
(70) Sapir, L.; Harries, D. Restructuring a Deep Eutectic Solvent by Water: The Nanostructure of Hydrated Choline Chloride/Urea. *J. Chem. Theory Comput.* **2020**, *16,* 3335-3342.
(71) D'Agostino, C.; Gladden, L. F.; Mantle, M. D.; Abbott, A. P.; Essa, I. A.; Al-Murshedi, A. Y.; Harris, R. C. Molecular and Ionic Diffusion in Aqueous–Deep Eutectic Solvent Mixtures: Probing Inter-Molecular Interactions Using Pfg Nmr. *Phys. Chem. Chem. Phys.* **2015**, *17,* 15297-15304.
(72) López-Salas, N.; Vicent-Luna, J. M.; Imberti, S.; Posada, E.; Roldán, M. a. J. s.; Anta, J. A.; Balestra, S. R.; Madero Castro, R. M.; Calero, S.; Jiménez-Riobóo, R. J. Looking at the "Water-in-Deep-Eutectic-Solvent" System: A Dilution Range for High Performance Eutectics. *ACS Sustainable Chem. Eng.* **2019**, *7,* 17565-17573.
(73) Hammond, O. S.; Bowron, D. T.; Edler, K. J. The Effect of Water Upon Deep Eutectic Solvent Nanostructure: An Unusual Transition from Ionic Mixture to Aqueous Solution. *Angew. Chem., Int. Ed.* **2017**, *56,* 9782-9785.
(74) Abbasi, N. M.; Farooq, M. Q.; Anderson, J. L. Investigating the Variation in Solvation Interactions of Choline Chloride-Based Deep Eutectic Solvents Formed Using Different Hydrogen Bond Donors. *ACS Sustainable Chem. Eng.* **2021**, *9,* 11970-11980.
(75) Meng, X.; Ballerat-Busserolles, K.; Husson, P.; Andanson, J.-M. Impact of Water on the Melting Temperature of Urea + Choline Chloride Deep Eutectic Solvent. *New J. Chem.* **2016**, *40,* 4492-4499.
(76) Nishi, N.; Yamazawa, T.; Sakka, T.; Hotta, H.; Ikeno, T.; Hanaoka, K.; Takahashi, H. How Viscous Is the Solidlike Structure at the Interface of Ionic Liquids? A Study Using Total Internal Reflection Fluorescence Spectroscopy with a Fluorescent Molecular Probe Sensitive to High Viscosity. *Langmuir* **2020**, *36,* 10397-10403.

(77) Abbasi, N. M.; Farooq, M. Q.; Anderson, J. L. Investigating the Effect of Systematically Modifying the Molar Ratio of Hydrogen Bond Donor and Acceptor on Solvation Characteristics of Deep Eutectic Solvents Formed Using Choline Chloride Salt and Polyalcohols. *J. Chromatogr. A* **2022**, *1667,* 462871.
(78) Farooq, M. Q.; Odugbesi, G. A.; Abbasi, N. M.; Anderson, J. L. Elucidating the Role of Hydrogen Bond Donor and Acceptor on Solvation in Deep Eutectic Solvents Formed by Ammonium/Phosphonium Salts and Carboxylic Acids. *ACS Sustainable Chem. Eng.* **2020**, *8,* 18286-18296.
(79) Ludes, M. D.; Wirth, M. J. Single-Molecule Resolution and Fluorescence Imaging of Mixed-Mode Sorption of a Dye at the Interface of C18 and Acetonitrile/Water. *Anal. Chem.* **2002**, *74,* 386-393.

TOC Figure

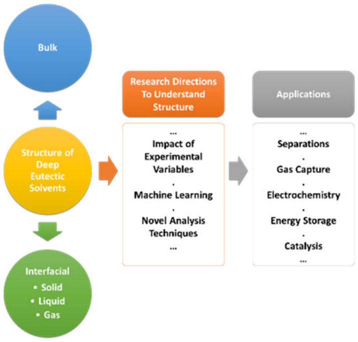
Bulk
Structure of Deep Eutectic Solvents
Interfacial
• Solid
• Liquid
• Gas
Research Directions To Understand Structure
...
Impact of Experimental Variables
.
Machine Learning
.
Novel Analysis Techniques
...
Applications
...
Separations
.
Gas Capture
.
Electrochemistry
.
Energy Storage
.
Catalysis
...

Author Biographies

Emily A. Smith

Emily Smith is a Professor of Chemistry at Iowa State University and the Division Director for Chemical and Biological Sciences at Ames National Laboratory, a US Department of Energy national laboratory. She received her Ph.D. from University of Wisconsin-Madison in 2003. She was a postdoc at University of Delaware and she was a Ruth L. Kirschstein National Research Service Award (NIH) Postdoctoral Fellow at the University of Arizona and the Arizona Cancer Center. Her research interests are optical spectroscopy instrument development for the analysis of nanoscale phenomena and materials.

Nicole M. Stephens

Nicole Stephens is an Assistant Professor of Chemistry at Wartburg College. She received her Ph.D. from Iowa State University in 2022. Her research interests include chemical education and optical spectroscopy.